

Viscosity alpha in rotating spherical shear flows with an external magnetic field

A. Drecker¹, R. Hollerbach² and G. Rüdiger¹

¹ *Astrophysikalisches Institut Potsdam, An der Sternwarte 16, D-14482 Potsdam, Germany*
adr@aip.de, gruediger@aip.de

² *Department of Mathematics, University of Glasgow, Glasgow, G12 8QW, UK*
rainer@maths.gla.ac.uk

Accepted Received ; in original form 1997

ABSTRACT

We study the turbulent behaviour induced by the magnetic shear instability for a magnetized, incompressible fluid in a spherical shell. A differential rotation which is decreasing outwards but hydrodynamically stable according to the Rayleigh criterion is prescribed, and an external, uniform magnetic field is imposed parallel to the rotation axis. Our main concern in this paper will be the fully global treatment of this magnetohydrodynamical system, so we focus particular attention on the influence of the boundary conditions. Nonlinear, steady solutions are presented for both stress-free as well as for rigid boundary conditions for one specific model with a fixed strength of the external magnetic field and a fixed differential rotation rate. We calculate the eddy viscosity ν_T and the viscosity alpha α_{SS} resulting from the total stress tensor. These turbulence parameters turn out to differ drastically depending on the boundary conditions for the flow. A parametric transition from the magnetic shear instability to the hydrodynamical instability shows that the enhanced generation of turbulence takes place mainly in the boundary layers of the shell.

Key words: instabilities – MHD – turbulence – shear flow – viscosity alpha

1 MOTIVATION

It is still one of the key questions in astrophysics to explain how turbulence can be generated in astrophysical bodies. Molecular viscosity is usually estimated to be too small to solve the problem of angular momentum transport, for example in accretion discs. Moreover, putting this question into the context of magnetohydrodynamics, it is also related to dynamo theory since turbulent flows of conducting fluids can provide appropriate mechanisms for self-sustained magnetic fields due to the underlying complex field structures. If one takes into account the presence of magnetic fields turbulence could be driven by magnetohydrodynamical instabilities.

Recently, considerable effort has been spent on the investigation of the magnetic shear instability, which was originally discovered independently by Velikhov (1959) and Chandrasekhar (1960) for Couette flow. Nowadays it is often called ‘Balbus-Hawley’ instability, because they were the first to realize its significance in astrophysics when they applied it to accretion disks (Balbus & Hawley 1991, 1994). Their linear analysis has shown that a weak magnetic field (rather than a strong one) can cause a destabilizing effect

for angular velocity profiles which are decreasing outwards with the radius, even when the differential rotation is stable according to the Rayleigh criterion of pure hydrodynamics. The generation of turbulence in the nonlinear regime was demonstrated by Brandenburg et al. (1995), Hawley et. al (1995) and Matsumoto & Tajima (1995). But most of these investigations have been restricted to a local analysis using a Cartesian box. On the other hand, linear studies (Curry & Pudritz 1995, Kitchatinov & Mazur 1997) have revealed a strong dependence of the instability growth rates on the boundary conditions.

A global linear analysis for a differentially rotating magnetized sphere of an incompressible fluid was performed by Kitchatinov & Rüdiger (1997). Their findings were that rotation laws sub-critical to the Rayleigh stability criterion produce an instability in a finite interval of the magnetic field amplitude. The upper bound of this interval is imposed by the finite size of the system. The analysis yielded the existence of a region in parameter space where nonaxisymmetric modes are preferred which might be important for the occurrence of a dynamo effect due to the theorem of Cowling (1934).

The plan of the present paper is as follows: At first the

magnetohydrodynamical system under investigation is described. After some remarks about the numerical approach we show the results of a linear stability analysis which have been obtained by a truncated version of the code. In the case of rigid boundary conditions the effect of preferred nonaxisymmetric modes disappears.

For the nonlinear simulations in this study we have chosen a specific model in parameter space where linear analysis does not elucidate which modes will actually be excited. The resulting solutions, which turn out to be axisymmetric and steady, are used to calculate the radial structure of the eddy viscosity and the viscosity alpha. Shakura and Sunyaev (1973) have stated the hypothesis that the latter parameter be constant, which has now become a widespread assumption for constructing accretion disk models. In the case of stress-free boundary conditions the diagrams for both parameters do not show any typical turbulent behaviour. For rigid boundary conditions we do indeed find a range where that parameter is constant, with the exception of the vicinity of the inner and outer boundaries. Furthermore, the value of this level appears to be independent of the slope of the differential rotation law, whereas the effect of enhanced turbulence due to increased shear is restricted to the boundary layers.

2 THE MODEL

2.1 Mathematical formulation

We consider a spherical shell of conducting, incompressible fluid with inner radius R_i and outer radius R_o which is embedded in vacuum. Since there are no thermodynamics included in our model we supplement the MHD equations by some kinematically prescribed differential rotation $\mathbf{u}_0 = \boldsymbol{\Omega} \times \mathbf{r}$, where the rotation law

$$\boldsymbol{\Omega} = \frac{\Omega_0 \mathbf{e}_z}{\sqrt{1 + (\varpi/\varpi_0)^{2q}}}. \quad (1)$$

depends only on the distance $\varpi = r \sin \theta$ to the rotation axis. The parameter ϖ_0 is given by $\varpi_0 = (R_o - R_i)/2$. An external uniform magnetic field $\mathbf{B}_0 = B_0 \mathbf{e}_z$ is imposed parallel to the rotation axis. The instabilities of this flow have previously been considered in the linear regime for stress-free boundary conditions by Kitchatinov and Rüdiger (1997). The parameter q determines the hydrodynamic stability according to the Rayleigh criterion $\Omega d(\varpi^2 \Omega)/d\varpi \geq 0$ (see for example Chandrasekhar (1961)), with $q \leq 2$ corresponding to stability. The resulting velocity profile is decreasing with radius, which is necessary for the Balbus-Hawley instability to occur (Balbus & Hawley 1991). Length and time are normalized with respect to the difference in radii and the magnetic diffusion time,

$$\mathbf{r} = (R_o - R_i) \mathbf{r}', \quad t = \frac{(R_o - R_i)^2}{\eta} t'. \quad (2)$$

For the normalization of the fluid flow we do not use the ratio length-scale/time-scale, but instead the prescribed differential rotation.

$$\mathbf{u} = (R_o - R_i) \Omega_0 \mathbf{u}'. \quad (3)$$

We normalize the magnetic field strength as

$$\mathbf{B} = \sqrt{4\pi\rho}(R_o - R_i) \Omega_0 \mathbf{B}' \quad (4)$$

in order to make the Lorentz and inertia forces comparable. Furthermore we split up the total magnetic field into the external field \mathbf{B}_0 and the dynamical magnetic fields \mathbf{B}' which are governed by the induction equation. Both values are related by a Hartmann-like number. Thus it is possible to switch off the external field by decreasing the Hartmann number (7). Expressed in terms of these dimensionless variables (the dashes have been omitted afterwards again) the momentum and the induction equations then become

$$\frac{\partial \mathbf{u}}{\partial t} - \text{Pm} \Delta \mathbf{u} = -\nabla p + C_\Omega \mathbf{u} \times (\nabla \times \mathbf{u}) \quad (5)$$

$$+ C_\Omega \mathbf{u}_0 \times (\nabla \times \mathbf{u}) + C_\Omega \mathbf{u} \times (\nabla \times \mathbf{u}_0) \\ + C_\Omega (\nabla \times \mathbf{B}) \times \mathbf{B} + \text{Ha} (\nabla \times \mathbf{B}) \times \mathbf{B}_0,$$

$$\frac{\partial \mathbf{B}}{\partial t} - \Delta \mathbf{B} = C_\Omega \nabla \times (\mathbf{u} \times \mathbf{B}) \quad (6)$$

$$+ C_\Omega \nabla \times (\mathbf{u}_0 \times \mathbf{B}) + \text{Ha} \nabla \times (\mathbf{u} \times \mathbf{B}_0),$$

where the parameters

$$\text{Pm} = \frac{\nu}{\eta}, \quad C_\Omega = \frac{\Omega_0 (R_o - R_i)^2}{\eta}, \quad \text{Ha} = \frac{(R_o - R_i) B_0}{\sqrt{4\pi\rho}\eta} \quad (7)$$

are the magnetic Prandtl number, the dynamo number, which is a measure of the angular velocity of the differential rotation, and the Hartmann number. Our Hartmann number differs only by a factor of $\sqrt{\text{Pm}}$ from that of Kitchatinov & Rüdiger. Since we are going to consider only the case $\text{Pm} = 1$ in this study, we can make a comparison with their linear results as another test of our time-stepping code. Since both vectors \mathbf{u} and \mathbf{B} are divergence-free they can be represented by toroidal and poloidal components (Chandrasekhar, 1961; Krause & Rädler 1980)

$$\mathbf{u} = \mathbf{r} \times \nabla \left(\frac{\Phi}{r} \right) + \nabla \times \left(\mathbf{r} \times \nabla \left(\frac{\Psi}{r} \right) \right), \quad (8)$$

$$\mathbf{B} = \mathbf{r} \times \nabla \left(\frac{B}{r} \right) + \nabla \times \left(\mathbf{r} \times \nabla \left(\frac{A}{r} \right) \right). \quad (9)$$

It is convenient to expand the scalar potentials A, B, Ψ and Φ into spherical harmonics, the eigenfunctions of the Laplacian Δ on the 2-sphere, e.g.

$$A = \sum_{l,m} A_{lm} P_l^{|m|}(\cos \theta) e^{im\phi}. \quad (10)$$

The pressure in the Navier-Stokes equation (5) can be eliminated by taking the curl which yields the vorticity transport equation. The following equations for the coefficients govern the dynamical behaviour of our model system

$$\sum_{l,m} \frac{l(l+1)}{r^2} \left(\frac{\partial}{\partial t} - D^2 \right) A_{lm} P_l^m e^{im\phi} = \mathbf{e}_r \cdot \nabla \times \mathbf{E}, \quad (11)$$

$$\sum_{l,m} \frac{l(l+1)}{r^2} \left(\frac{\partial}{\partial t} - D^2 \right) B_{lm} P_l^m e^{im\phi} = \mathbf{e}_r \cdot \nabla \times \nabla \times \mathbf{E}, \quad (12)$$

$$\sum_{l,m} \frac{l(l+1)}{r^2} \left(\frac{\partial}{\partial t} - D^2 \right) \Phi_{lm} P_l^m e^{im\phi} = \mathbf{e}_r \cdot \nabla \times \mathbf{F}, \quad (13)$$

$$\sum_{l,m} \frac{l(l+1)}{r^2} \left(\frac{\partial}{\partial t} - D^2 \right) D^2 \Psi_{lm} P_l^m e^{im\phi} = -\mathbf{e}_r \cdot \nabla \times \nabla \times \mathbf{F}, \quad (14)$$

where

$$D^2 = \frac{\partial^2}{\partial r^2} - \frac{l(l+1)}{r^2} \quad (15)$$

denotes the effective angular momentum operator and

$$\begin{aligned} \mathbf{E} &= C_\Omega(\mathbf{u} \times \mathbf{B}) + C_\Omega(\mathbf{u}_0 \times \mathbf{B}) \\ &+ \text{Ha}(\mathbf{u} \times \mathbf{B}_0), \end{aligned} \quad (16)$$

the total electromotive force (EMF). The forcing \mathbf{F} for the Navier-Stokes equation is given by

$$\begin{aligned} \mathbf{F} &= C_\Omega \mathbf{u} \times (\nabla \times \mathbf{u}) \\ &+ C_\Omega \mathbf{u}_0 \times (\nabla \times \mathbf{u}) + C_\Omega \mathbf{u} \times (\nabla \times \mathbf{u}_0) \\ &+ C_\Omega (\nabla \times \mathbf{B}) \times \mathbf{B} + \text{Ha}(\nabla \times \mathbf{B}_0) \times \mathbf{B}. \end{aligned} \quad (17)$$

2.2 Boundary conditions

We consider both stress-free as well as rigid boundary conditions for the flow. In the former case the cross-components $\pi_{r\phi}$, $\pi_{r\theta}$ of the viscous stress-tensor $\pi_{ij} = -\rho\nu(u_{i,j} + u_{j,i})$ have to vanish, which can be expressed by the scalar potentials Ψ and Φ as follows:

$$\frac{2}{r} \frac{\partial \Psi_{lm}}{\partial r} - \frac{\partial^2 \Psi_{lm}}{\partial r^2} = 0, \quad \frac{\partial}{\partial r} \left(\frac{\Phi_{lm}}{r^2} \right) = 0 \quad (18)$$

In the latter case all components of the flow have to vanish at the surface. This condition yields

$$\frac{\partial \Psi_{lm}}{\partial r} = 0, \quad \Phi_{lm} = 0. \quad (19)$$

In both cases no normal flow on the radial component is imposed at $r = r_i, r_o$ which simply implies the vanishing of Ψ at the boundary

$$\Psi_{lm} = 0. \quad (20)$$

Taking the regions $r < r_i$ and $r > r_o$ to be insulators, the vacuum boundary conditions for the magnetic field become:

$$\frac{\partial A_{lm}}{\partial r} - \frac{l+1}{r} A_{lm} = 0 \quad \text{at} \quad r = r_i, \quad (21)$$

$$\frac{\partial A_{lm}}{\partial r} + \frac{l}{r} A_{lm} = 0 \quad \text{at} \quad r = r_o, \quad (22)$$

$$B_{lm} = 0 \quad \text{at} \quad r = r_o, r_i. \quad (23)$$

2.3 Numerical approach

The spectral expansion for the coefficients is completed by using Chebyshev polynomials $T_k(x)$ for the radial structure

$$A_{lm}(r) = \sum_k a(k, l, m) T_{k-1}(x), \quad (24)$$

where the radius r is mapped to the interval $[-1, 1]$ via

$$r = \frac{r_o + r_i}{2} + \frac{r_o - r_i}{2} x. \quad (25)$$

The equations (11–14) are then time-stepped as follows: all terms appearing on the right-hand sides are treated explicitly, and are evaluated pseudospectrally. Having thus separated out the spectral coefficients of these terms, one can time-step the equations separately for each l and m . This is done by treating the terms on the left-hand sides implicitly, and results in a series of $K \times K$ matrix equations, where K is the number of Chebyshev polynomials one is using.

See also Hollerbach (1997) for a complete description of the numerical method. For our simulations we have used the following numerical resolution: 30 Chebyshev polynomials, 30 Legendre functions and 5 harmonics. In order to make the effects of the inner hole (which is included only for computational convenience) negligible, we fixed the radius ratio to $r_i/r_o = 1/5$. With these truncations, and at dynamo numbers of around $C_\Omega = 1000$, the code runs stably with a time-step of around $\delta t = 5 \times 10^{-5}$. A single time-step on an HP-735 workstation then requires approximately 6 seconds of CPU-time.

3 RESULTS AND DISCUSSION

By truncating the code to a linear version we have obtained Figs 1 and 2 for the case $q = 2$ in the C_Ω –Ha plane. Fig 1 shows the neutral stability lines for the symmetric and anti-symmetric (concerning the symmetry of the magnetic fields with respect to the equatorial plane) modes $m = 0, 1$ when stress-free boundary conditions have been imposed on the flow. In this case there exists a region for higher Hartmann numbers where the excitation of nonaxisymmetric modes is preferred, in agreement with the results of Kitchatinov & Rüdiger (1997). According to the theorem of Cowling (1934) this could be relevant for the existence of a self-consistent dynamo.

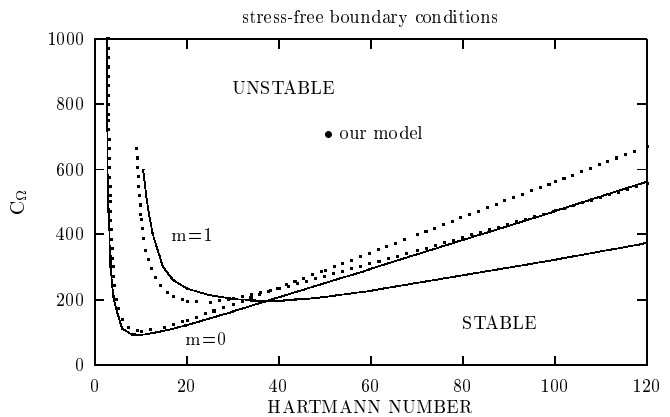


Figure 1: The lines of neutral stability in the case of stress-free boundary conditions reveal a region where nonaxisymmetric modes are preferred. This agrees with Figs 7 and 8 of Kitchatinov & Rüdiger (1997). The lines for symmetric (antisymmetric) modes are plotted with full (dotted) lines. The symbol \bullet shows the location of our model in the parameter space.

Fig 2 shows the neutral stability lines when rigid boundary conditions have been imposed. In this case the excitation of axisymmetric modes is always preferred. Note, though, that this is largely due to the fact that the lines for $m = 1$ have shifted up considerably; the lines for $m = 0$ are remarkably unchanged. Despite this similarity in the $m = 0$ lines, however, the corresponding eigenfunctions do show quite different behaviour close to the boundaries.

For the nonlinear analysis we restricted ourselves to the point $\text{Ha} = 50$, $C_\Omega = 714$ in parameter space. Since this

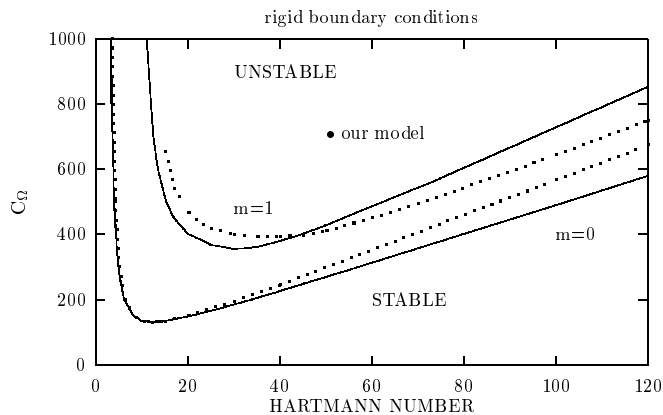


Figure 2: The lines of neutral stability in the case of rigid boundary conditions. Axisymmetric modes are always preferred.

point is located above the neutral stability lines for all four modes, symmetric and antisymmetric $m = 0, 1$, these linear diagrams do not tell which modes will actually be present in the nonlinear solution, and how strong they will be. The reason for choosing this particular point $\text{Ha} = 50$, $C_\Omega = 714$ is that at this point the nonlinear solutions still turn out to be purely axisymmetric, and indeed purely antisymmetric, for both stress-free as well as rigid boundary conditions. Choosing this point for our model thus ensures that the overall structure of the system will be comparable for both boundary conditions. Figs. 3 and 4, which show the structure of the flow and the total magnetic field, exhibit the dipole character of the solution. The z -component of the external field is amplified by a factor of four at the inner boundary. The ratio of kinetic to magnetic energies $E_{kin}/E_{mag} \approx 3.5$ shows that these models are still dominated by the flow.

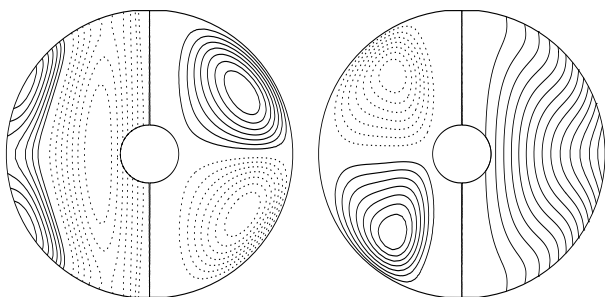


Figure 3: The field structure for stress-free boundary conditions. From left to right: contour plot of u_ϕ , streamlines of the meridional flow, isolines of the total toroidal magnetic field, and the field lines of the total poloidal magnetic field. Full lines refer to positive contour lines resp. clockwise circulation.

Using the data from these nonlinear simulations we proceed to study the turbulent behaviour of our model. Since all the solutions are steady the analysis of the data requires no time average. We begin by investigating the eddy viscosity which relates the total horizontal stress to the large-scale

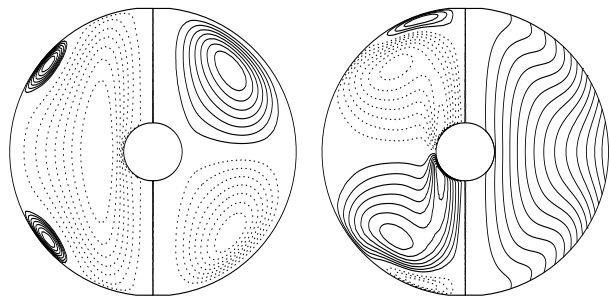


Figure 4: The same as on Fig. 3, but for rigid boundary conditions. The strongest influence of the boundary conditions can be observed by comparing the boundaries of the toroidal fields.

shear and which is a measure for the efficiency of the angular momentum transport. In our nondimensionalized units the prescription for the calculation of the ratio of eddy and molecular viscosity ν_T/ν reads

$$\langle u_r u_\phi - B_r B_\phi \rangle = -\frac{\nu_T}{\nu} \cdot \frac{\text{Pm}}{C_\Omega} \varpi \left(\frac{d\Omega}{d\varpi} \right) \quad (26)$$

The right-hand side of (26) is evaluated at the equatorial plane. The averaging scheme for the correlation tensor, consisting of the Maxwell and the Reynolds parts, uses an integration over the variables θ and ϕ , but keeps the dependence on the radius. The full line in Fig. 5 shows the eddy viscosity ν_T related to the molecular viscosity ν for rigid boundary conditions. For this case we find a typical “turbulent” behavior of ν_T , the main contribution coming from a peak at $\nu_T \approx 13$ close to the inner hole. The eddy viscosity is positive throughout the whole shell (except the region $0.8 \leq r \leq 0.9$, but the corresponding values of ν_T are insignificantly small), which means that angular momentum is transported outwards. This should be contrasted with purely hydrodynamical simulations for accretion disks (Cabot & Pollack 1991; Stone & Balbus 1996) which have yielded that the mean Reynolds stress arising from turbulent convection is negative. These authors have therefore concluded that Rayleigh-stable flows cannot display any outwards directed transport. In the case of stress-free boundary conditions the rather small values indicate that there is *no effective mechanism* for angular momentum transport in our model.

In many turbulence models it has been assumed that the viscosity alpha $\nu_T = \alpha_{SS} \Omega H^2$ is constant. Here the scale height $H(\varpi) = \sqrt{r_o^2 - \varpi^2}$ above the equatorial plane was introduced (Ω and H are again taken in this definition at $\theta = \pi/2$). For rigid boundary conditions (6) we find that there exists a region $0.3 < r < 0.7$ where this parameter has the constant value $\alpha_{SS} \approx 3 \times 10^{-3}$, justifying the hypothesis of Shakura and Sunyaev. We again find a peak for α_{SS} at the inner boundary. Except for a small region above $r = 0.8$ this parameter is positive and tends to infinity at the outer boundary due to the vanishing scale height H . For stress-free boundary conditions this is not true, instead the values are one order of magnitude smaller and there is no constant region. Furthermore the parameter changes its sign above $r = 0.8$.

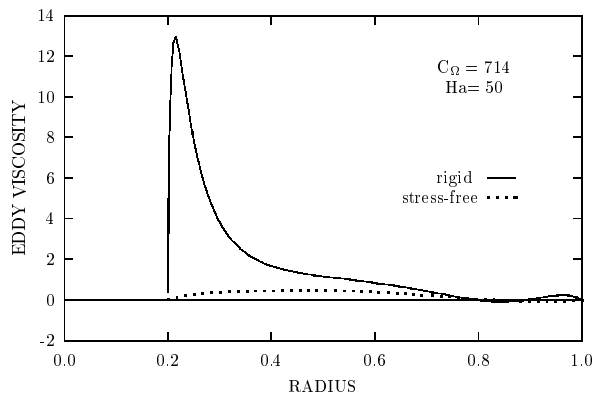


Figure 5: The ratio of eddy and molecular viscosity resulting from the total stress tensor has a strong peak at the inner boundary in the case of rigid boundary conditions. For stress-free boundary conditions the values are much smaller and show no significant behaviour.

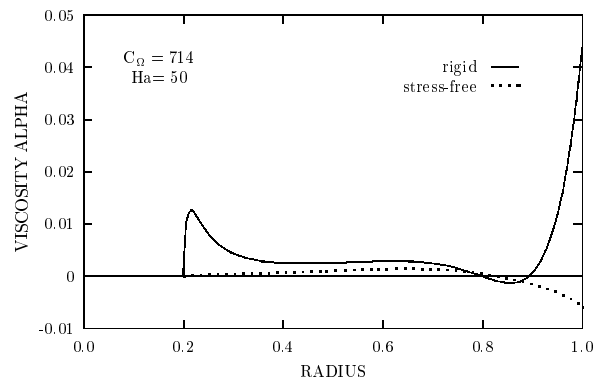


Figure 6: The radial dependence of the viscosity alpha for rigid boundary conditions peaks close to the inner hole of the shell. The constant level in the middle appears to be independent of variations in the parameter q . Again, the behaviour for stress-free boundary conditions is completely different.

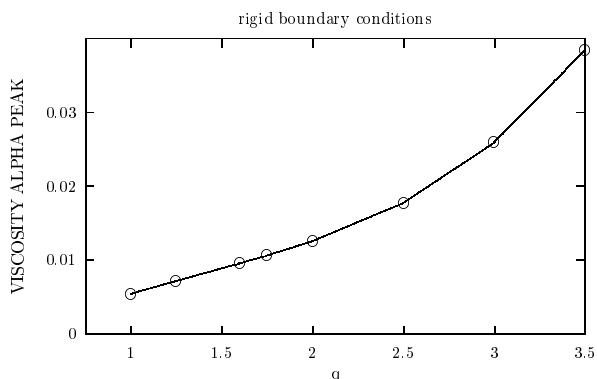


Figure 7: The peak of the viscosity alpha as a function of the parameter q of the differential rotation. The curve is linear in the range $1 \leq q \leq 2$. After the transition to the hydrodynamically unstable regime the viscosity alpha increases strongly.

The last investigation is concerned with the influence of the slope of the differential rotation law on the viscosity alpha. Abramowicz et al. (1996) calculated the viscosity alpha (averaged over the whole volume of a local shearing box) in accretion disks when a power law like $\Omega \sim r^{-q}$ holds for the differential rotation. They found that the Shakura-Sunyaev parameter becomes infinite for the case $q = 2$. From that fact they suggested that the viscosity alpha increases linearly with the shear-vorticity ratio. Even though they used simulations with dynamo-generated rather than externally imposed fields, it is worth noting that we found no singular behaviour at $q = 2$, since in general the only effect of an external magnetic field will be to increase the value of the Shakura-Sunyaev parameter. We have varied the parameter q for our model in the range from 1.0 to 3.5. Fig. 7 seems to reveal a linear relation between the maximum of α_{SS} and q until a critical point $q \approx 2$ where hydrodynamical instability sets in. Beyond that point the values for α_{SS} are growing rapidly, but they remain finite. Moreover, the height of the plateau in the middle of the shell is unaffected by the variations in q , so that the effect of enhanced turbulence by increased shear is restricted to the boundary layers.

4 CONCLUDING REMARKS

In this paper we have discussed numerical solutions for the fully global treatment of the magnetic shear instability in spherical geometry. Therefore, the study is especially aimed at the question how the turbulent behaviour of the flow is affected by the choice of different boundary conditions. As a first result it was shown that the linear analysis yields already drastic differences concerning the excitation of the eigenmodes. So far only one specific nonlinear model in the parameter space has been considered. The main outcome from these nonlinear simulations is that the turbulent parameters, the eddy viscosity and the Shakura-Sunyaev parameter, are rather sensitive to the boundary conditions of the flow. The linear analysis predicts for stress-free boundary conditions and appropriate dynamo- and Hartmann numbers the preferred excitation of nonaxisymmetric modes. The theorem of Cowling encourages us therefore to do a more thorough survey of the parameter space as the next step.

REFERENCES

- Abramowicz M., Brandenburg A., Lasota J.-P., 1996, MNRAS, 281, L21-L24
- Balbus S. A., Hawley J. F., 1991, ApJ, 376, 214
- Balbus S. A., Hawley J. F., 1994, MNRAS, 266, 769
- Balbus S. A., 1995, ApJ, 453, 380
- Brandenburg A., Nordlund Å., Stein R. F., Torkelsson U., 1995, ApJ, 446, 741
- Cabot W., Pollack J. B., 1991, Geophys. Astrophys. Fluid Dyn., 64, 97
- Chandrasekhar S., 1961, Hydrodynamic and Hydromagnetic Stability. Clarendon, Oxford
- Cowling T. G., 1934, MNRAS, 94, 39
- Curry C., Pudritz R. E., Sutherland P. G., 1994, ApJ, 434, 206
- Curry C., Pudritz R. E., 1995, ApJ, 453, 697
- Curry C., Pudritz R. E., 1996, MNRAS, 281, 119
- Hawley J. F., Balbus S. A., 1991, ApJ, 376, 223

- Hawley J. F., Gammie C. F., Balbus S. A., 1995, *ApJ*, 440, 742
Hollerbach R., (in preparation)
Kitchatinov L. L., Rüdiger G., 1997, *MNRAS*, 286, 757
Kitchatinov L. L., Mazur M. V., 1997, *A&A*, in press
Krause F., Rädler K.-H., 1980, *Mean-Field Magnetohydrodynamics and Dynamo Theory*. Akademie-Verlag, Berlin
Matsumoto R., Tajima T., 1995, *ApJ*, 445, 767
Rüdiger G., 1989, *Differential Rotation and Stellar Convection: Sun and Solar-Type Stars*. Gordon & Breach, New York
Shakura N. I., Sunyaev R. A., 1973, *A&A*, 24, 337
Stone J. M., Balbus S. A., 1996, *ApJ*, 464, 364-372
Velikhov E. P., 1959, *Sov. Phys. JETP*, 9, 995